VOL. 9, NO. 7, JULY 2014 ISSN 1819-6608
ARPN Journal of Engineering and Applied Sciences


www.arpnjournals.com

STABILIZATION OF ACTIVE MAGNETIC BEARING SYSTEM USING SINGLE NEURON PID CONTROLLER

Polamraju.V. S. Sobhan[1], G. V. Nagesh Kumar[2], J. Amarnath[3] and M. Subbarao[1]
[1]Vignan University, Vadlamudi, Guntur, Andhra Pradesh, India
[2]GITAM University, Visakhapatnam, Andhra Pradesh, India
[3]JNTUH, Andhra Pradesh, India
E-Mail: pvssobhan@gmail.com

ABSTRACT

This paper presents the development and implementation of a hybrid controller to automatically levitate and precisely regulate the position of a suspended rotor in Active Magnetic Bearing system. The inherent nonlinearity and open-loop instability of AMBs present challenges for design a controller and the problem can be formulated as a dynamic, multivariable optimization problem. A single neuron adaptive PID controller which is different from conventional PID controller with constant gains is designed by combining single neuron structure with PID mechanism. The ability of self-learning and adaptive of ANN and the robustness of PID control retained in the proposed SNPID controller. It can adjust weighting parameters to retain the desired performance automatically. The simulation results show that using SNPID controller designed via PSO algorithm exhibits superior robustness compared to PID controlled systems.

Keywords: active magnetic bearing, single neuron, PID controller, PSO.

1. INTRODUCTION

Active Magnetic Bearings (AMBs) provide non-contacting support of high speed rotating shaft in an air-gap within the motor using electro magnetic forces. The AMBs are unique alternative to the problems experienced in traditional mechanical bearing systems like frequent lubrication, bearing friction, high energy dissipation, limited rotational speed etc. Active magnetic bearing systems have tremendous potential for many areas such as jet engines, compressors, turbomolecular vacuum pumps, semiconductor manufacturing equipments, flywheel energy storage systems and other high speed rotating machinery [1, 2]. Constructionally active magnetic bearing systems are much larger in size due to the additional complex control circuitry, sensors, actuators and required power supplies [3].

The significant drawback of these systems is difficult to design a controller due to its uncertainty, highly nonlinear dynamics and inherent instability [4]. The controller has to actively control electromechanical forces that support the rotor to control the motion of a rotor and can be used to damp out unbalance responses of a rotor in stator. The most useful approach of dealing such a nonlinear system is to linearize it about a single nominal equilibrium point and then use linear control technique. The zero-radial-force point at the centre of the stator core is an unstable point so that negative feedback is necessary. A well-identified mathematical model is necessary for this inherently unstable AMB system [5, 6].

The controller design for active magnetic bearing system is a difficult task due to the instability and destabilization of the rotor. This is particularly a challenging problem since damping is extremely weak due to contact less levitation and since the poles are displaced by gyroscopic effects when the rotor is rotating.

To obtain robust performance, we propose a hybrid controller, which is the combination of PID control, Artificial Neural Network and optimization technique.

2. MODELING OF AN ACTIVE MAGNETIC BEARING SYSTEM

2.1. One-DOF modeling

The basic structure of a differential type of magnetic actuator for one-axis magnetic suspension is shown in Figure-1. The cylindrical rotor suspended in the air between two C-shaped electromagnets by a controlled magnetic force can move in the x direction. For uniform flux distribution in the air gap between both sides of the rotor, B+ and B- are the flux densities in air gaps respectively. The air gap area is S with a sum of S_1 andS_2. The magnetic forces F_+ and F- are applied to the cylindrical object are

$$F_+ = \frac{S}{2\mu_0} B_+^2 \text{ and } F_- = \frac{S}{2\mu_0} B_-^2 \quad (1)$$

The sum of these magnetic forces F is written as

$$F = F_+ - F_- = \frac{S}{2\mu_0}(B_+^2 - B_-^2) \quad (2)$$

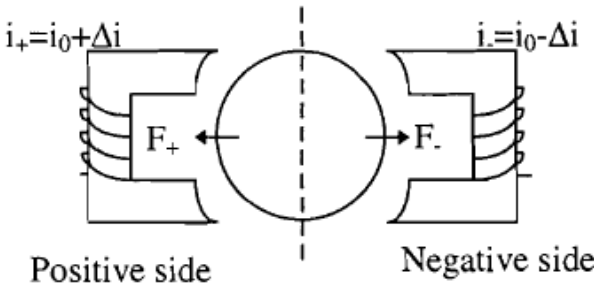

Figure-1. Differential actuator.

It can be seen that the magnetic force in either direction is proportional to the difference of flux density squared.

2.2. Two -DOF modeling

A typical Active magnetic bearing with two degree of freedom and its cross sectional view is shown in Figure-2. The cylindrical rotor shaft is located at the center and is surrounded by eight electro magnets made of ferromagnetic material such as laminated silicon steel. The magnetic paths of the eight stator poles complete through the stator yoke. To avoid vibration caused by radial magnetic forces and to increase mechanical stiffness the width of the stator yoke is designed to be wide enough and it also avoids magnetic saturation.

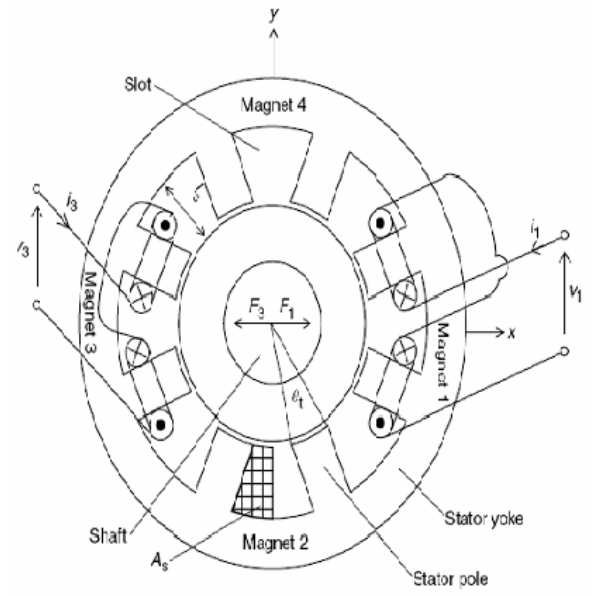

Figure-2. Radial magnetic bearing.

Magnets 1 to 4 are formed with the eight poles and each magnet two stator poles are wound with two short pitch coils. These coils are connected in series so that only two terminals are required for one magnet. The two magnets 1 and 3 are working in differential mode to generate a radial force in x-direction i.e. Magnet 1 levitates the rotor in the x-axis (+x-axis) direction where as magnet 3 levitates in the opposite (−x-axis) direction. Similarly Magnets 2 and 4 produce y-axis radial force also in differential mode. The generated radial forces in two directions i.e. x-axis and y-axis forces by four magnets which are operating in differential mode can be regulated independently by controlling the currents flowing through them.

The generated radial force in one direction by two stator poles with an angular position of 22.5 deg, between poles is given by (3)

$$F = \frac{B_0^2}{2\mu_0} s \cos(\frac{\pi}{8}) \quad (3)$$

Here S = area of one stator pole in air gap is given by

$$S = l(\pi D \times \frac{\theta_t}{360}) \quad (4)$$

Where

D = rotor outer diameter (m)
l = stack length of a rotor core, i.e., rotor axial length (m)
θ_t = stator pole arc angle (deg)

The self-inductance of one electromagnet with a nominal air gap length of g is

$$L_0 = \frac{N^2 \mu_0 S}{2g} \quad (5)$$

Where N is the sum of the number of turns of two short-pitch coils.
The radial force becomes

$$F = \frac{L_0}{2g} \cos(\frac{\pi}{8}) i^2 \quad (6)$$

If F_1 and F_3 are the radial forces acting on the rotor in +x and –x directions, due to currents i_1 and i_3 then the net radial forces acting on the rotor in x- direction is given by

$$F_{xi} = F_1 - F_3 = K_i'(i_1^2 - i_3^2) \quad (7)$$

Where $K_i' = \frac{L_0}{2g} \cos(\frac{\pi}{8})$ (8)

If x is the displacement of the rotor from the centre position of rotor the unstsble force generated by electromagnets 1 and 3 are given by

$$F_{1u} = \frac{L_0}{g^2} i_1^2 x \cos(\frac{\pi}{8}) \text{ and } F_{2u} = \frac{L_0}{g^2} i_3^2 x \cos(\frac{\pi}{8}) \quad (9)$$

The non linear relationship between the radial force and the current components is realized by dividing the magnet winding currents i_1 and i_3 into two components i.e. bias current I_b and force regulating current i_b

$$i_1 = I_{bx} + i_{bx} \text{ and } i_3 = I_{bx} - i_{bx} \quad (10)$$

$$F_{xi} = K_i \, i_{bx} \quad (11)$$

From (11) by regulating current i_{bx} the radial force can be regulated.

The total unstable radial force generated in the direction of x-axis is

$$F_{xu} = K_x \, x \quad (12)$$

Where $K_x = \frac{2L_0 \cos(\frac{\pi}{8})}{g^2} I_b^2$ (13)

The net radial force generated in x-axis direction F_x is a function of both the current i_{bx} and rotor radial displacement x. The radial force F_x is the sum of these forces

$$F_x = k_i i_{bx} + k_x x \quad (14)$$

The lineralized mechanical dynamic equation of the AMB in the direction of x-axis with a rotor mass m (kg) is given by (15) and its block diagram representation is shown in Figure-3.

$$m\ddot{x} = k_i \, i_{bx} + k_x \, x \quad (15)$$

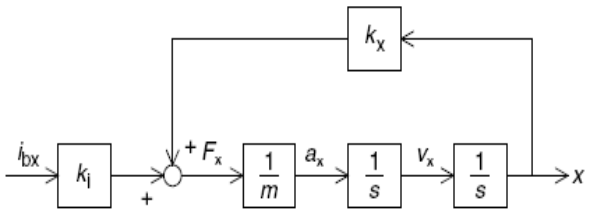

Figure-3. Block diagram of magnetic suspension system.

The two radial forces generated are aligned usually coincide with the x- and y-axis displacements. The radial force misalignment results in interference of x- and y-axis force components because of the following reasons

a) A delay in the radial force due to eddy currents flux
b) The gyroscopic effect in short-axial-length and large radius rotor machines.
c) The error in the estimated angular positioning of the revolving magnetic field

Figure-4 shows the block diagram of the two axis AMB system that includes the interference of x- and y-axis force components.

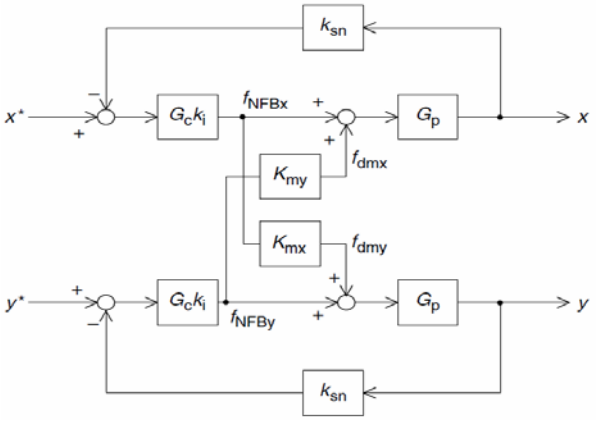

Figure-4. Interference in two-axis magnetic suspension.

The interference radial forces f_{dmx} and f_{dmy} can be expressed as functions of feedback radial forces f_{NFBx}, f_{NFBy} and direction angle error θ_{er} in (16)

$$f_{dmx} = K_{mx} \, f_{NFB\,y} \text{ and } f_{dmy} = K_{my} \, f_{NFB\,x} \quad (16)$$

Where $K_{mx} = -\sin\theta_{er}$, $K_{my} = \sin\theta_{er}$ (17)

3. SINGLE NEURON PID CONTROLLER

Single neuron PID adaptive controller has abilities of self-adapting and self-learning and nonlinear reflection as well as good robustness and its simple structure. The sensitivity to parameter variations of conventional PID control is minimized by combining with intelligent control. The single neuron PID controller has better learning ability and ensures that the system can get better control effect under external disturbances [7-10].

By choosing adaptive weighting parameters of neuron model the undesirable performance of response due to changes in parameters and their accuracies can be corrected automatically. However in these systems the challenge is to choose an appropriate neuron proportional coefficient A that is the most sensitive parameter.

A single neuron adaptive PID control system is represented by the block diagram in Figure-5. The controller implements functions of adaptive and

algorithms of self-learning by adjusting weighting parameter $W_1(k)$, $W_2(k)$ and $W_3(k)$. The modification of the weighting parameters is achieved by supervised Hebb self-learning Rule

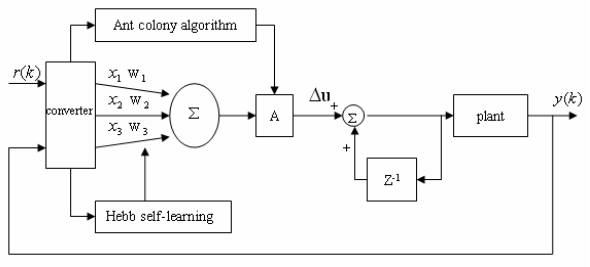

Figure-5. Block diagram of a single neuron adaptive PID control system.

The error between the two inputs of converter i.e. desired input $r(k)$ and actual output $y(k)$ is used for generation of three outputs $x_1(k), x_2(k)$ and $x_3(k)$ which acts as inputs of the single neuron circuit

$$x_1(k) = e(k) \tag{18}$$

$$x_2(k) = \Delta e(k) = e(k) - e(k-1) \tag{19}$$

$$x_3(k) = \Delta^2 e(k) = e(k) - 2e(k-1) + e(k-2) \tag{20}$$

$$z(k) = e(k) = r(k) - y(k) \tag{21}$$

According to increment type PID algorithm, the output of single neuron can be written as

$$u(k) = u(k-1) + A\sum_{i=1}^{3} W_i^{'}(k)\, x_i(k) \tag{22}$$

And its learning algorithm is

$$W_i^{'}(k) = \frac{W_i(k)}{\sum_{i=1}^{3} |W_i(k)|} \qquad (i = 1,2,3) \tag{23}$$

$$W_1(k) = W_1(k-1) + \lambda_I\, z(k)\, u(k)\, x_1(k) \tag{24}$$

$$W_2(k) = W_2(k-1) + \lambda_P\, z(k)\, u(k)\, x_2(k) \tag{25}$$

$$W_3(k) = W_3(k-1) + \lambda_D\, z(k)\, u(k)\, x_3(k) \tag{26}$$

Where

$\lambda_P =$ Proportional element learning rate

$\lambda_I =$ Integrate element learning rate

$\lambda_D =$ Derivative element learning rate and

$A =$ Neuron proportional coefficient, $A > 0$.

The three learning rates λ_P, λ_I, λ_D can be adjusted simultaneously by changing neuron proportional coefficient *A* which is the most sensitive parameter in the system, if *A* is too small, it will need a long response time. The supervising Hebb learning algorithm is used to calculate the changes in weights of a neural network in which a change in the strength of a neuron connection is a function of the pre- and post- synaptic neural activities.

The neuron connection strength between the output of the pre-synaptic neuron x_1 and the output of the post-synoptic neuron x_2 is expressed as

$$W_{ij}(t) = \lambda\, x_1 * x_2 \tag{27}$$

Where λ learning rate.

4. SIMULATION AND RESULTS

4.1. Simulation of single neuron adaptive PID (SNPID) controller

The MATLAB/ SIMULINK model of single neuron adaptive PID controller for an AMB system is shown in Figure-6. The input to the single neuron adaptive PID controller (SNPID) is the error between the reference input and actual output and the SNPID output is the actuating signal applied to the plant. The error between the reference input and actual output is used for generation of three outputs $x_1(k), x_2(k)$ and $x_3(k)$

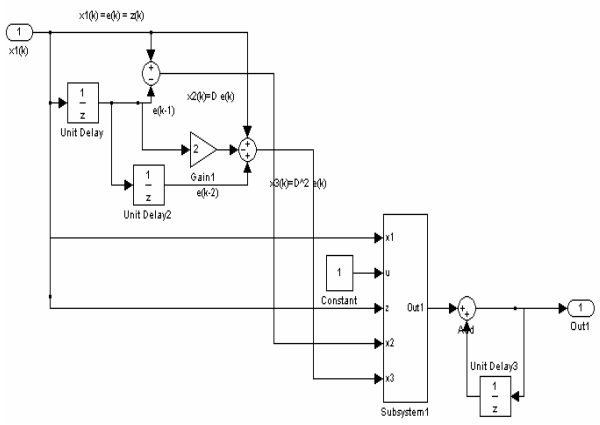

Figure-6. Simulation model of SNPID controller.

The subsystem for generating actuating signal $u(k)$ using the weighting parameters $W_1(k)$, $W_2(k)$ $W_3(k)$ and it's updating according to supervised Hebb self-learning Rule is shown in Figure-7 and Figure-8.

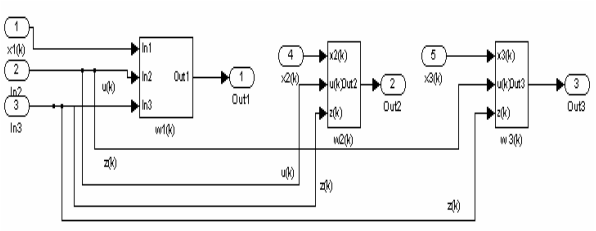

Figure-7. Simulated model for generating the weighting parameters W_1, W_2, W_3 using $x_1(k)$, $x_2(k)$ and $x_3(k)$.

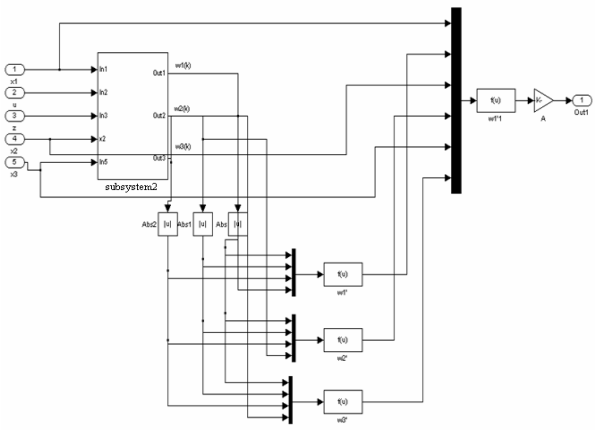

Figure-8. The subsystem using the weighting parameters W_1, W_2, W_3 and it's updating according to supervised Hebb self-learning rule.

The AMB system parameter values and the tuned constants of Single Neuron PID controller are shown in Table-1.

Table-1. Parameters of the AMB system and SNPID controller.

Parameter	Optimum values
Mass of the rotor	3.14 kg
Radius of the stator	0.09 m
Length of the rotor	0.15m
Air gap length	2mm
Force displacement factor	170000 N/m
Moment of inertia along x-axis	0.016 Kg m^2
Moment of inertia along y-axis	0.00023 Kg m^2
Force current factor	158N/A
λ_I	0.35
λ_P	25
λ_D	550
A	1000

4.2. 1-DOF AMB system

1-DOF Active magnetic bearing system with SNPID controller is modeled in MATLAB/SIMULINK is shown in Figure-9.

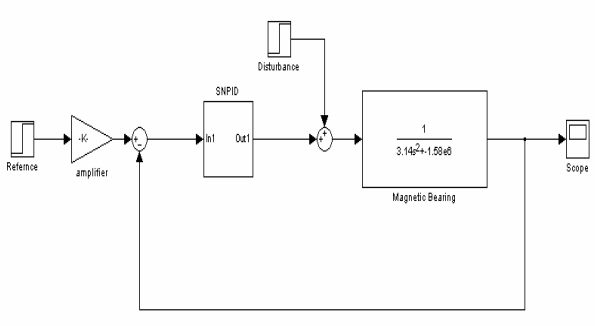

Figure-9. 1-DOF Active magnetic bearing system with SNPID controller.

The simulation results for 1-DOF AMB system with PID and Single Neuron PID controllers is shown in the Figure-10. and it can be observed that both the controllers makes the AMB system stable and the SNPID controller gives better transient and steady state response than the conventional PID controller.

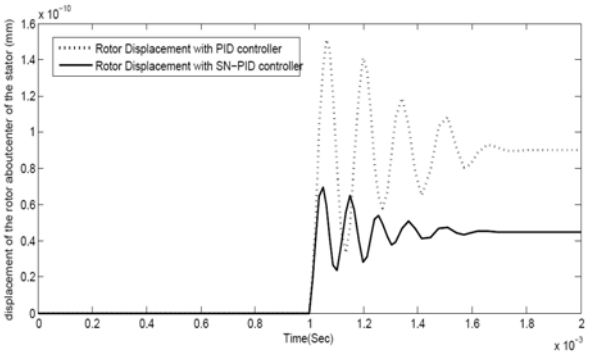

Figure-10. Comparison of responses of SNPID and PID controllers for 1-DOF AMB system.

4.3. 2-DOF AMB system

Simulation of 2-DOF Active magnetic bearing system with PID and SNPID controllers using MATLAB/SIMULINK is shown in Figure-11 and Figure-12.

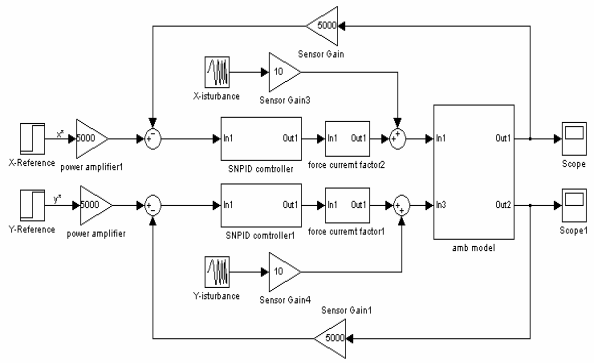

Figure-11. 2-DOF Active magnetic bearing system with SNPID controller.

The simulation results for 2-DOF AMB system with SNPID and Conventional PID controllers for the displacement of rigid rotor in the directions of both X-axis and Y-axis is shown in the Figure-12.

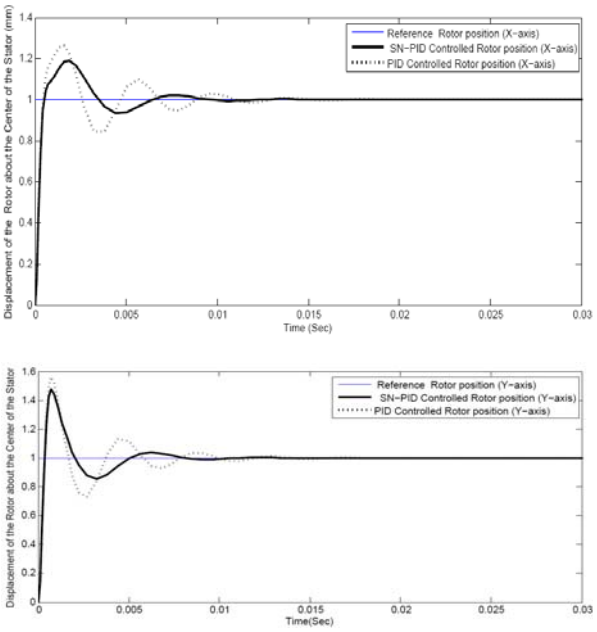

Figure-12. Comparison of responses of SNPID and PID controllers for 2-dof AMB system in the directions of both X-axis and Y-axis.

From Figure-12 it can be observed that the SNPID controller gives better transient and steady state response than the conventional PID controller. The SNPID controller reduces the peak over shoot from 28% to 18%, settling time from 0.014 to 0.008 sec for X-axis displacement and peak over shoot from 58% to 48%, settling time from 0.014 to 0.008 sec for Y-axis displacement.

The Simulation results for 2-DOF AMB system with SNPID and Conventional PID controllers for the displacement of rigid rotor in the directions of both X-axis and Y-axis for variable reference input is shown in the Figure-13

The reference value is zero from 0 sec to 0.02 sec then it is increased to 0.5 and continued up to 0.04 sec further it is increased to unity.

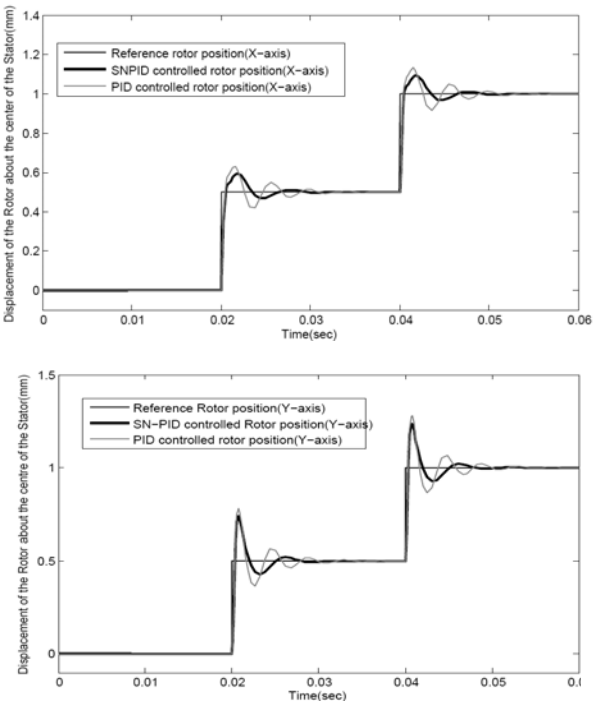

Figure-13. Comparision of responses of SNPID and PID controllers for 2-dof AMB system in the directions of both X-axis and Y-axis at variable reference input.

From Figure-13 it can be observed that the SNPID controlled output tracks variable reference input than the conventional PID controller.

5. CONCLUSIONS

This paper introduced the working way of Active magnetic Bearings (AMBs) and a detailed linear model was developed using analytic relationships. In order stabilize the AMB and to damp shaft vibrations due to unbalance forces, a controller that integrates the merits of traditional PID control and artificial neuron with the abilities of self-adapting and self-learning is proposed. The designed SNPID controller is applied to both 1-DOF and 2-DOF active magnetic bearing models. The incorporation of the developed single neuron adaptive PID controller in to the existing AMB system has given effective results. The simulation results show that the reduction of overshoot, shorter

REFERENCES

[1] G. Schweitzer, H. Bleuler and A. Traxler. 1994. Active Magnetic Bearings - Basics, Properties and Applications of Active Magnetic Bearings. vdf Hochschulverlag AG an der ETH Zuerich.

[2] M. Dussaux. 1990. The industrial applications of active magnetic bearing technology. Proceedings of the 2nd International Symposium on Magnetic Bearings, July 12- 14. pp. 33-38.

[3] C. E. Lin and H. L. Jou. 1993. Force model identification for magnetic suspension systems via magnetic-field measurement. IEEE Transactions on Instrumentation and Measurement. pp. 767-771, April.

[4] K.Y. Lum, T. Coppola and S. Bemstein. 1996. Adaptive Autocentering Control for an active Magnetic Bearing Supporting a Rotor with Unknown Mass Imbalance. IEEE Trans. on Control Systems Technology. 14(5): 687-597.

[5] A. Charara J.D. Miras and B. Caron. 1996. Nonlinear control of a Magnetic Levitation System without Premagnetization. IEEE Trans. on Control systems Technology. 14(5): 513-523.

[6] J. Levine, J. Lotton and J.C. Ponsart. 1996. A nonlinear approach to the control of magnetic bearings. IEEE Transactions on Control Systems Technology. 4(5): 524-544.

[7] Y. Zhenyu and G. Pedersen. 2006. Automatic tuning of PID controller for a 1-D levitation system using a genetic algorithm - A real case study. Proceedings of the IEEE International Symposium on Intelligent Control. pp. 3098-3103.

[8] L. Li. 1996. On-line tuning of AMB controllers using genetic algorithms. In: Proc. 6th Int. Symp Magnetic Bearings. Cambridge, MA: Mass. Inst. Technol., August 5-7. pp. 372-382.

[9] I.A. Griffin, A.J. Chipperfield and P.j. Fleming. 2000. Active Magnetic Bearing Control System Testing and Validation Using a Multi-objective Genetic Algorithm. Trans. IEEE, June. pp. 1675 -1679.

[10] Z. Xiu and G. Ren. 2004. Optimization design of TS-PID fuzzy controllers based on genetic algorithms. Proceedings of the 5th World Congress on intelligent Control and Automation, Hangzhou, China. pp. 2476-2480, June.